Engineering Journal issn: 0125-8281

Article

Synthesis of Light Hydrocarbons via Oxidative Coupling of Methane over Silica-supported Na_2WO_4-TiO_2 Catalyst

Anusorn Seubsai[1,2,3], Palida Tiencharoenwong[1], Phattaradit Kidamorn[1], and Chalida Niamnuy[1,3,*]

1 Department of Chemical Engineering, Faculty of Engineering, Kasetsart University, Bangkok 10900, Thailand
2 Center of Excellence on Petrochemical and Materials Technology, Kasetsart University, Bangkok 10900, Thailand
3 Research Network of NANOTEC–KU on NanoCatalysts and NanoMaterials for Sustainable Energy and Environment, Kasetsart University, Bangkok 10900, Thailand
*E-mail: fengcdni@ku.ac.th (Corresponding author)

Abstract. Methane is of great interest for conversion into high-value hydrocarbons (C_{2+}) and olefins, via oxidative coupling of methane (OCM) using catalysts. In this work, Na_2WO_4-TiO_2/SiO_2 catalyst, along with the single catalysts of its components (Na_2WO_4/SiO_2 and TiO_2/SiO_2), was investigated for OCM reaction to C_{2+}. We found that 5 wt% Na_2WO_4+ 5 wt% TiO_2 on the SiO_2 support was a superior catalyst for OCM reaction compared to the single catalysts. The maximum C_{2+} formation of the Na_2WO_4-TiO_2/SiO_2 catalyst was found under test conditions of a N_2/($4CH_4$:$1O_2$) feed gas ratio of 1:1, a reactor temperature of 700 ºC, and gas hourly space velocity of 9,500 h^{-1}, exhibiting 71.7% C_{2+} selectivity, 6.8% CH_4 conversion, and 4.9% C_{2+} yield. Moreover, the activity of the catalyst had good stability over 24 h of on-stream testing. The characterizations of the Na_2WO_4-TiO_2/SiO_2 catalyst using XRD, FT-IR, XPS, FE-SEM, and TEM revealed that a crystalline structure of α-cristobalite of SiO_2 was present along with TiO_2 crystals, substantially enhancing the activity of the catalyst for OCM reaction to C_{2+}.

Keywords: Catalyst, light hydrocarbons, oxidative coupling of methane, sodium tungsten oxide, titanium oxide.

ENGINEERING JOURNAL Volume 23 Issue 5
Received 28 March 2019
Accepted 10 June 2019
Published 30 September 2019
Online at http://www.engj.org/
DOI:10.4186/ej.2019.23.5.169

This article is based on the presentation at The 8th International Thai Institute of Chemical Engineering and Applied Science Conference (ITIChE2018) in Chonburi, Thailand, 8th-9th November 2018.

DOI:10.4186/ej.2019.23.5.169

1. Introduction

Methane (CH_4) is the main compound of biogas and natural gas that are plentiful on Earth. It is considered a greenhouse gas with an environmental impact more than 25 times greater than CO_2 if equal amounts of these two gases are released into the atmosphere. Since methane is an abundant compound on Earth, a process that can convert methane to high value-added chemicals is a highly attractive topic for many researchers. One of the challenging topics to be considered in catalysis is oxidative coupling of methane (OCM)—a gas-phase reaction that uses O_2 or air to directly react with CH_4 to produce useful hydrocarbons (C_{2+}) such as ethylene, ethane, propane, and propylene [1, 2]. The OCM reaction is an exothermic reaction in nature and normally takes place at reaction temperatures of 600–1,000 ºC [3]. OCM can produce CO and CO_2 as byproducts. However, if a suitable catalyst is present, the reaction produces a selective product and extreme reaction temperatures can be reduced.

In the past several years, some potential catalysts have been reported, including MnO_x modified with different types of co-catalysts, supports and promotors, such as oxides of Mg, Na, and Ce. However, the C_{2+} yields and C_{2+} selectivities were quite low at approximately <16% and 25-78%, respectively [4-8]. Additionally, coke formation was found during the reaction, resulting in catalyst deactivation. Later, the coking formation was, however, prevented by introducing of chlorinated compounds with the reactant gases. Alternatively, a binary catalyst of Na_2WO_4-MnO_x has been widely investigated because this metal combination was identified as an active material for the OCM reaction. The modified Na_2WO_4-MnO_x catalysts reported include MO_x-Na_2WO_4-MnO_x/SiO_2 (M = Ni, Co, Fe, Li, Al, Ba, Ca, Na, and K) [9], TiO_2-Na_2WO_4/MnO_x/SiO_2 [10], and Ce_2O_3-MnO_x-Na_2WO_4/SiO_2 [7]. The C_{2+} yields and C_{2+} selectivities of those Na_2WO_4-MnO_x catalysts increased compared to the single catalysts of its component and the other metal combinations due to synergistic catalyst effects between Na_2WO_4 and MnO_x [11-14]. The additions of the promoters (e.g. TiO_2, Ce_2O_3) onto the Na_2WO_4-MnO_x catalysts resulted in improved activity of the catalysts, because the promoters could cooperate into the catalytic materials and/or the number of suitable strong basic sites increased [15, 16]. Normally, SiO_2 is used as a catalyst support because the SiO_2 support is stable under the test conditions and inert to the products [14].

Since previous results reported in the literatures showed that any catalysts containing Na_2WO_4, MnO_x, and/or SiO_2 are highly active for OCM reaction, it is of great interest and challenging to improve new catalysts that consist of any of those components and new active metal component (i.e co-active metal, promoter). In a catalyst screening for OCM reaction in our laboratory, we discovered that addition of TiO_2 onto the Na_2WO_4/SiO_2 catalyst without MnO_x can also substantially improve the C_{2+} yield. This combination of TiO_2 and Na_2WO_4 on SiO_2 has never been reported in detail. Herein, we report on various studies on the activity of Na_2WO_4 mixed with TiO_2 on SiO_2 support. The studies include catalyst optimization, catalyst stability, operating condition for the reaction, and catalyst characterization.

2. Experimental Section

2.1. Catalyst Preparation

All of the catalysts were synthesized using co-impregnation of predetermined weights of SiO_2 as follows. An aqueous solution of Na_2WO_4 (sodium tungstate dihydrate, 98.0~101.0%, Daejung) and Ti^{4+}(titanium (IV) isopropoxide, 97+%, Alfa Aesar) in ethanol (99.9%, QREC) were determined and pipetted into amorphous fume silica (SiO_2, surface area of 85-115 m^2/g, Alfa Aesar) to obtain a desired weight percentage of the metal components (TiO_2 and/or Na_2WO_4) on the SiO_2 support. Note that the weight percentage of TiO_2 or Na_2WO_4 on the support was determined on the basis of the mass of Ti(0) or Na_2WO_4, respectively. The mixture was continuously stirred at 120 ºC until dry. The obtained powder was then taken to calcine in an air furnace at 800 ºC for 4 h. After the calcination, a fine white powder was obtained.

2.2. Catalyst Activity Test

The activities of the prepared catalysts were evaluated for OCM reaction in a plug flow reactor at 1 atm and a reactor temperature range of 600–800 ºC. A sample (8 mg) was packed in a quartz tubular reactor that had an inner diameter of 0.5 cm. The catalyst bed length was approximately 2 mm and the catalyst was

sandwiched between two layers of quartz wool. The feed gas consisted of nitrogen (N_2, 99.999% purity, Praxair), methane (CH_4, 99.999% purity, Praxair), and oxygen (O_2, 99.999% purity, Praxair) at a volume ratio of (N_2:CH_4:O_2) = (0–7.5):4:1 (i.e. fixing the volume ratio of CH_4:O_2 = 4:1) with a total feed flow rate of 50 mL/min, which corresponded to a gas hourly space velocity (GHSV) of 9,500 h^{-1}. The effluent gas was analysed using a gas chromatograph (Shimadzu, GC-14A) equipped with a thermal conductivity detector (TCD; for analyzing CO, CO_2, and CH_4) and a flame ionization detector (FID; for analysis of C_2H_4, C_2H_6, C_3H_6, C_3H_8 and C_4H_8, and C_4H_{10}). The catalytic activities are expressed in terms of %CH_4 conversion, %C_{2+} selectivity, %CO_x selectivity, and %C_{2+} yield, which are shown in Eq. (1)–(4). The data were collected after the system had reached the set point for 2h.

$$\%\ CH_4\ \text{conversion} = \frac{\text{moles of } CH_4 \text{ input - moles of } CH_4 \text{output}}{\text{moles of } CH_4 \text{ input}} \times 100 \tag{1}$$

$$\%\ C_{2+}\ \text{selectivity} = \frac{\text{moles of } C_{2+}}{\text{Total moles of products}} \times 100 \tag{2}$$

$$\%\ CO_x\ \text{selectivity} = \frac{\text{moles of } CO_x}{\text{Total moles of products}} \times 100 \tag{3}$$

$$\%\ C_{2+}\ \text{yield} = \frac{\%\ CH_4 \text{conversion} \times \%\ C_{2+} \text{selectivity}}{100} \tag{4}$$

2.3. Catalyst Characterization

The patterns of powder X-ray diffraction (XRD) the samples were received using a powder X-ray diffractometer (PXRD; X-Pert, Philips and JDX-3530, JEOL) with using Cu-K_a radiation with 40 mA and 45 kV, 0.5 s step time, 0.02° step size.

The pore volumes, pore-sizes, and specific surface areas of the samples were evaluated using N_2-physisorption with a Quantachrome Autosorp-1C instrument and Brunauer-Emmett-Teller (BET) procedure at a temperature of −196 °C.

The surface morphology of the samples was imaged using a field emission scanning electron microscope (FE-SEM, JSM7600F, JEOL) with an energy dispersive X-ray spectrometer (EDS), operated at 300 kV). Each sample was coated by gold (Au) using Au sputtering technique.

The particles at the nano-scale of the catalysts were characterized using a high-resolution transmission electron microscope (HR-TEM, JEM-3100F, JEOL) performed at 300 kV.

The Fourier-transform infrared (FT-IR) patterns of the samples were acquired using an FT-IR spectrometer (TENSOR2, Bruker, attenuated total reflection (ATR) mode). For the measurements, fine powder of each catalyst was mixed with potassium bromide (KBr), and then made into a KBr pellet.

The electronic states of sodium, tungsten, and titanium were analyzed using X-ray photoelectron spectroscope (XPS, Axis Ultra DLD, Kratos) with Al Kα for the X-ray source.

The metal-support and metal-metal interactions were analyzed using the H_2-temperature programmed reduction (H_2-TPR) technique. The H_2-TPR profiles of the samples were attained by carrying out the measurements in a tubular reactor (Inconel tube) in a temperature range of 50–900 °C with a heating rate of 5 °C/min. A gas mixture of 9.6% H_2 in Ar at a total feed flow rate of 30 mL/min was introduced into the sample bed. A TCD-equipped gas chromatography (GC-14, Shimadzu) was used to continuously monitor the H_2 consumption.

3. Results and Discussion

3.1. Activity of TiO_2/SiO_2, Na_2WO_4/SiO_2, and TiO_2-Na_2WO_4/SiO_2 Catalysts

The 10wt% TiO_2/SiO_2, 10wt% Na_2WO_4/SiO_2, and (5wt% TiO_2-5wt% Na_2WO_4)/SiO_2 catalysts were prepared and tested for OCM reaction, as presented in Fig. 1. The performance of each catalyst was described using the C_{2+} selectivity, CH_4 conversion, and C_{2+} yield. It should be noted that the C_{2+} yield is the criterion used to identify a superior catalyst when comparing the activities of catalysts. The C_{2+} yield of

the Na_2WO_4-TiO_2/SiO_2 catalyst was obtained at 2.7 %, clearly greater than that of the single TiO_2/SiO_2 or Na_2WO_4/SiO_2 catalysts, approximately 1.5 or 3.8 times the C_{2+} yield of the TiO_2/SiO_2 or Na_2WO_4/SiO_2 catalysts, respectively. However, the C_{2+} selectivity for these three catalysts was similar (approximately 39–42%) but the CH_4 conversion of the TiO_2/SiO_2 and Na_2WO_4/SiO_2 catalysts was lower than that of the Na_2WO_4-TiO_2/SiO_2 catalyst. The results indicated that the combination of TiO_2 and Na_2WO_4 on the SiO_2 support reveals a synergistic catalysis effect.

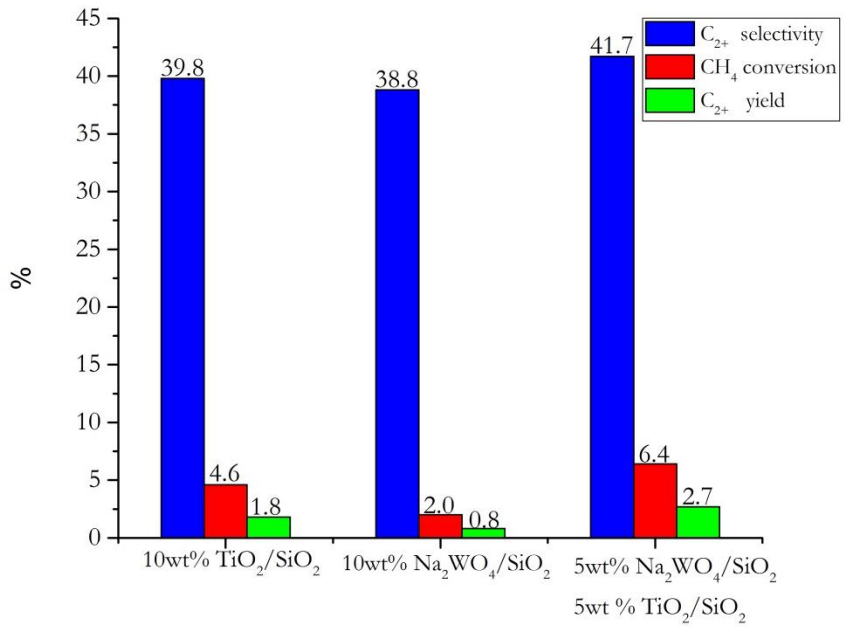

Fig. 1. C_{2+} selectivity, CH_4 conversion, and C_{2+} yield of 10wt% TiO_2/SiO_2, 10wt% Na_2WO_4/SiO_2, and TiO_2-Na_2WO_4/SiO_2 catalysts. Testing conditions: feeding gas ratio of CH_4:O_2 = 4:1 by volume, total feed flow rate = 50 mL/min (GHSV = 9,500 h^{-1}), and reactor temperature = 700 ºC.

3.2. Effect of TiO_2 Loading on Na_2WO_4-TiO_2/SiO_2

The Na_2WO_4-TiO_2/SiO_2 catalyst was further studied by varying the amount of TiO_2. In a previous study, 5wt% Na_2WO_4 loaded on SiO_2 using incipient-wetness impregnation was reported to produce an optimum yield for the OCM reaction [17]. However, the effect of TiO_2 loading on Na_2WO_4/SiO_2 has never been studied. In the present study, different amounts of TiO_2 on Na_2WO_4/SiO_2 were studied by varying the amounts of TiO_2 from 0 to 30% on the catalyst and keeping the amount of Na_2WO_4 on every catalyst unchanged at 5 wt%, as plotted in Fig. 2. As increasing TiO_2 loading, the C_{2+} selectivities slowly increased from 38.0 to 44.9%, while the CH_4 conversion steadily decreased from 6.4 to 4.3%. Nevertheless, the C_{2+} yield had an optimum yield at 5 wt% loading (2.7% C_{2+} yield). This confirmed that the addition of TiO_2 into Na_2WO_4/SiO_2 enhances C_{2+} formation. However, TiO_2 loadings over 5 wt% decreased the C_{2+} yield of each catalyst. Thus, Na_2WO_4-TiO_2/SiO_2 catalyst at a total metal loading of 10 wt% and a TiO_2:Na_2WO_4 weight ratio of 1:1 (i.e. 5 wt% Na_2WO_4 + 5 wt% TiO_2) was chosen for the optimum catalyst for further studies.

3.3. Effect of $N_2/(4CH_4{:}1O_2)$ Feeding Gas Ratio and Reactor Temperature

The optimal catalyst was further investigated at various $N_2/(4CH_4{:}1O_2)$ feeding gas ratios ($N_2/(4CH_4{:}1O_2)$ = 0.0–1.5) and reactor temperatures (600–800 ºC). For the previous studies in sections 3.1 and 3.2, the testing conditions were fixed at a CH_4:O_2 feeding gas ratio of 4:1 with a total feed flow rate of 50 mL/min (GHSV = 9,500 h^{-1}) without an inert gas at 700 ºC and atmospheric pressure. In this section, N_2 gas (a diluent gas) was co-fed with CH_4:O_2 by fixing the volume ratio of CH_4:O_2 = 4:1 and varying the volume ratio of N_2/CH_4:O_2 from 0.0 to 1.5, and also varying the reactor temperature from 600 to 800 ºC, while the

total feed flow rate was fixed at 50 mL/min. The C_{2+} yield, C_{2+} selectivity, and CH_4 conversion under each set of condition of the optimal catalyst are presented in Figs. 3(a), 3(b) and 3(c), respectively.

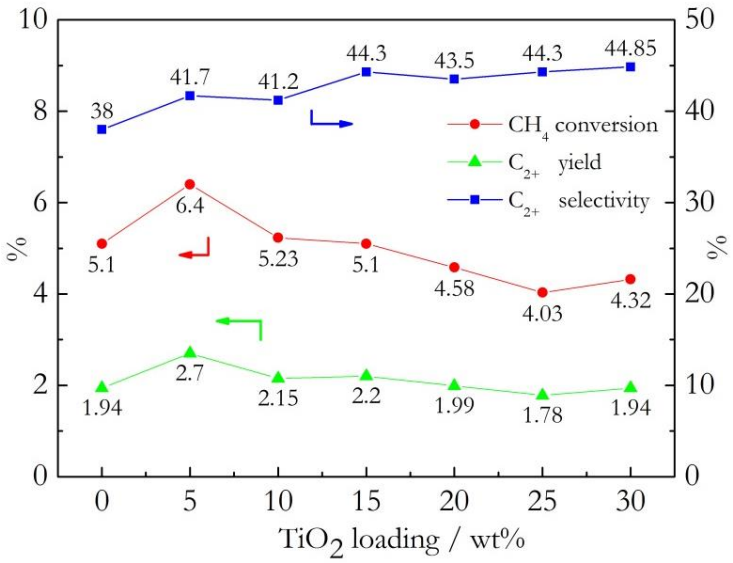

Fig. 2. TiO_2 loadings onto Na_2WO_4/SiO_2 from 0–30 wt% by fixing the amount of Na_2WO_4 onto each catalyst at 5 wt%; Testing conditions: feeding gas ratio of CH_4:O_2 = 4:1 by volume, total feed flow rate = 50 mL/min (GHSV = 9,500 h^{-1}), and reactor temperature = 700 °C.

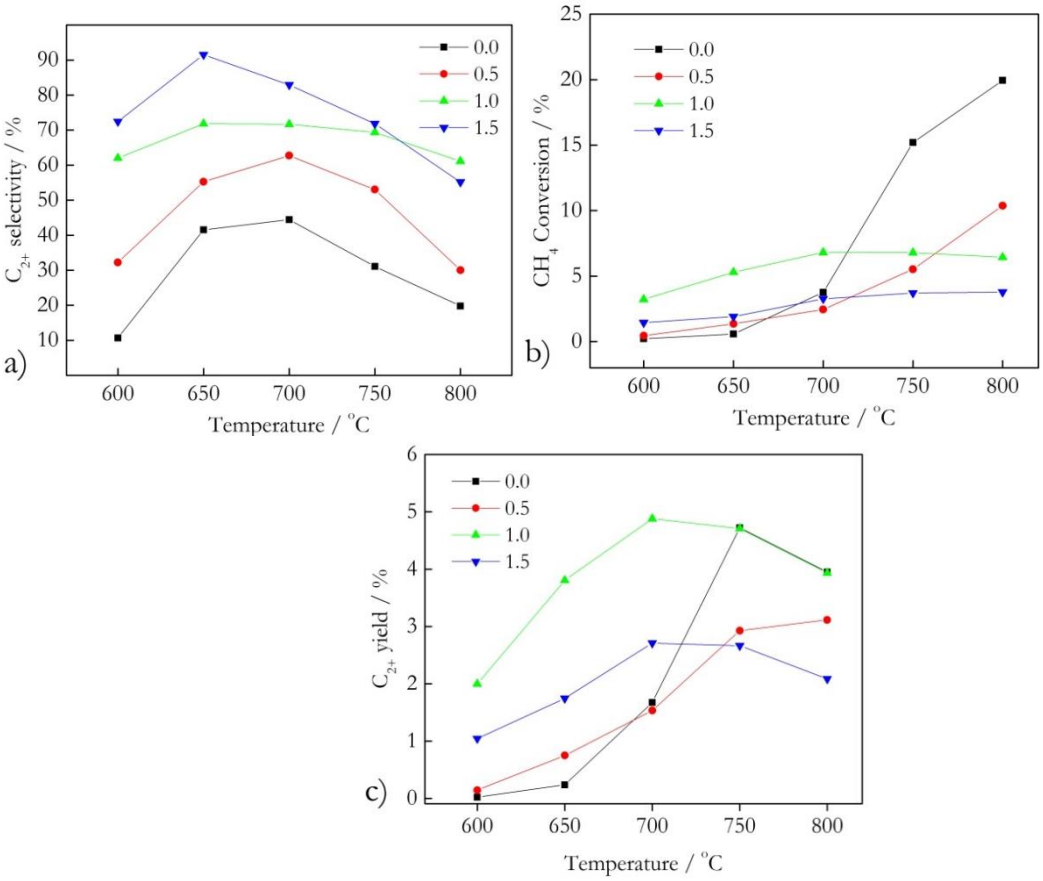

Fig. 3. a) C_{2+} selectivity, b) CH_4 conversion, and c) C_{2+} yield of the optimum TiO_2-Na_2WO_4/SiO_2 catalyst at $N_2/(4CH_4{:}1O_2)$ feeding gas ratios of 0.0–1.5 by volume, reactor temperatures of 600–800 °C, and total feed flow rate of 50 mL/min.

Comparing the C_{2+} selectivities at one reactor temperature (Fig. 3(a)), the C_{2+} selectivity mostly increased as the $N_2/(4CH_4{:}1O_2)$ feeding gas ratio increased. The maximum C_{2+} selectivity obtained was 91.5% with a $N_2/(4CH_4{:}1O_2)$ feeding gas ratio of 1.5 by volume and a reactor temperature of 650 ºC but the CH_4 conversion and the C_{2+} yield were low at 1.9% and 1.7%, respectively. However, the C_{2+} yield at every testing temperature decreased when the $N_2/(4CH_4{:}1O_2)$ feeding gas ratio was over 1.0 by volume because the reactant gases (i.e. CH_4 and O_2) were too diluted. In other words, the reactants were not sufficient for the active sites of the catalyst. In contrast, the C_{2+} yield of the $N_2/(4CH4{:}1O_2)$ feeding gas ratio of 0.0 and 0.5 was lower than that of 1.0 because the reactant gases were much more than the active sites and the heat generated by the catalytic reaction in the catalyst's bed was high, so that the products can further combust in the hotspot zone. Thus, the C_{2+} yields for these two conditions were relatively low.

Considering the catalytic activities at one $N_2/(4CH_4{:}1O_2)$ feeding gas ratio; the catalytic activities increased when the reactor temperatures was increased from 600 to 700 ºC. However, at reactor temperatures above 700 ºC, the C_{2+} selectivities decreased with increasing CH_4 conversion, and thus the overall C_{2+} production (i.e. C_{2+} yields) decreased because the combustion of CH_4 to CO_x products is favored at high reaction temperature [3], as well as the C_{2+} products being able to further react with some active species of the catalyst or to react with O_2 gas in the gas phase to further produce CO_x [18]. As seen in Fig. 3(c), the optimal C_{2+} yield was achieved at 4.9% with 71.7% C_{2+} selectivity and 6.8% CH_4 conversion when the operating conditions were an $N_2/(CH_4{:}O_2)$ feed gas ratio of 1.0 by volume and 700 ºC. These conditions were then chosen for a further study on the stability of the catalyst.

3.4. Catalytic Stability of Na_2WO_4-TiO_2/SiO_2

The catalytic stability of the Na_2WO_4-TiO_2/SiO_2 catalyst was investigated under the optimal conditions found in section 3.3. The activities of the catalyst over 24 h are presented in Fig. 4. Promisingly, the C_{2+} selectivities were high at approximately 69–71% during the testing period. However, the overall selectivity reduced by approximately 3% within 24 h. Moreover, the CH_4 conversions slowly decreased from 6.8 to 5.9, leading to decreased C_{2+} yield during the test period. It was also noticed that the CO_x selectivities gradually increased from 29 to 31%. The results suggested that the stability of the Na_2WO_4-TiO_2/SiO_2 catalyst was quite good for over 24 h. The slow deactivation of the catalyst requires further study, which is not the focus of this report.

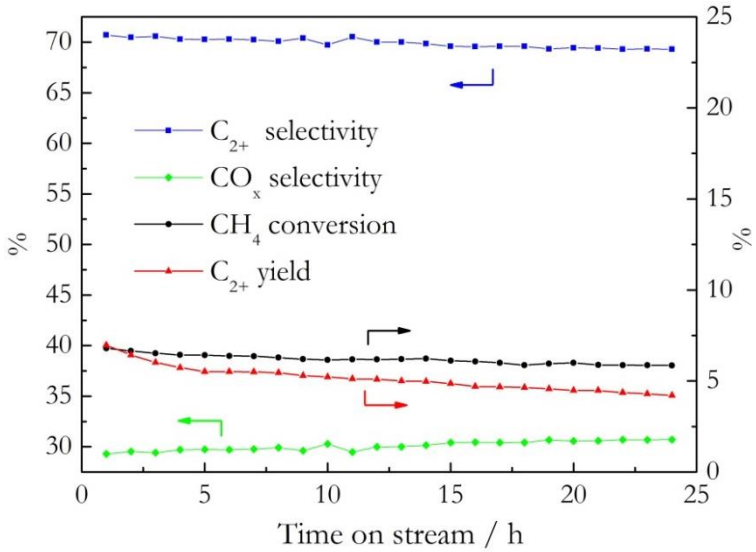

Fig. 4. Catalytic performance of Na_2WO_4-TiO_2/SiO_2 catalyst, testing conditions: $N_2/(4CH_4{:}1O_2)$ feeding gas ratio of 1.0, reactor temperature of 700 ºC, total feed flow rate of 50 mL/min, atmospheric pressure, and 24 h of testing.

3.5. Characterization of TiO_2/SiO_2, Na_2WO_4/SiO_2, and Na_2WO_4-TiO_2/SiO_2 Catalysts

The XRD pattern of the Na_2WO_4-TiO_2/SiO_2 catalysts compared with that of the TiO_2/SiO_2 and Na_2WO_4/SiO_2 catalysts are presented in Fig. 5. The TiO_2/SiO_2 catalyst exhibited two small peaks at 2θ of 25.2 and 48.5, indicating the presence of crystalline TiO_2 (anatase). It was also noticed that the SiO_2 support was in the amorphous phase. For the Na_2WO_4/SiO_2 catalyst, two crystalline compounds were observed. The first one was the crystalline Na_2WO_4, showing the characteristic peaks at 2θ of 7.16, 27.5, 32.4 and 48.4. The other was the presence of α-cristobalite (one of the crystalline forms of SiO_2), exhibiting the characteristic peaks at 2θ of 21.9, 28.3, 31.3, 36.0, 47.8, and 56.9. It was surprising to observe the formation of α-cristobalite at low a calcination temperature (800 ºC) in the presence of Na_2WO_4 because this crystalline form of SiO_2 normally occurs at calcination temperatures above 1,500 ºC [19]. Similarly, the α-cristobalite phase was observed in the Na_2WO_4-TiO_2/SiO_2 catalyst as clearly indicated by the characteristic XRD pattern. It was more interesting to observe that the characteristic peaks of TiO_2 were clearly seen for the Na_2WO_4-TiO_2/SiO_2 catalyst compared to those peaks in the Na_2WO_4-TiO_2/SiO_2 catalyst. This suggested that the environment in this catalyst enhanced the crystallinity of TiO_2. Thus, the important factor that promotes the formation of C_{2+} products of the Na_2WO_4-TiO_2/SiO_2 catalyst was the formation of the crystalline components (α-cristobalite, Na_2WO_4, and TiO_2).

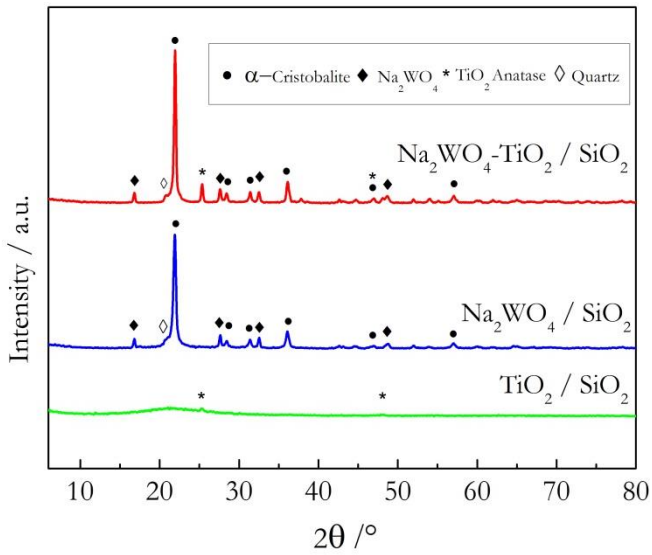

Fig. 5. XRD patterns of TiO_2/SiO_2, Na_2WO_4 /SiO_2, and Na_2WO_4-TiO_2/SiO_2.

The surface morphologies of the three catalysts imaged using FE-SEM were compared with the pure SiO_2 support and these are illustrated in Fig. 6(a)–Fig. 6(f). The SiO_2 support (Fig. 6(a)) and the TiO_2/SiO_2 catalyst (Fig. 6(b)) are similar, in that the particles are irregular in shape with sizes ranging from 20 to 50 nm. These particles were observed mostly in the amorphous SiO_2 support. The particles of the Na_2WO_4/SiO_2 catalyst (Fig. 6(c) and Fig. 6(d)) were also irregular in shape. Interestingly, the typical shape of the amorphous SiO_2 was completely transformed to a new shape, which was larger in size and possessed coral-reef like structures (approximately > 0.5 μm in diameter). This new structure was the crystalline α-cristobalite as identified by the XRD pattern. The Na_2WO_4-TiO_2/SiO_2 catalyst (Fig. 6(e) and Fig. 6(f) had similar the size and shape to the particles of the Na_2WO_4/SiO_2 catalyst. However, some small particles (approximately 50-100 nm in diameter) were observed throughout the catalyst. These particles were identified as TiO_2 crystals.

The TEM images of the Na_2WO_4-TiO_2/SiO_2 catalyst compared with those of the TiO_2/SiO_2 and Na_2WO_4/SiO_2 catalysts are shown in Fig. 7. The shape and size of each catalyst corresponded to the observation in the FE-SEM images (Fig. 6). The TEM images of the Na_2WO_4/SiO_2 (Fig. 7(c) and 7(d)) and Na_2WO_4-TiO_2/SiO_2 (Fig. 7(e) and 7(f)) catalysts confirmed that the amorphous SiO_2 support transformed to α-cristobalite when adding Na_2WO_4, in agreement with a previous report [20]. For the Na_2WO_4-

TiO_2/SiO_2 catalyst, crystalline TiO_2 particles were clearly observed with sizes ranging between 50 and 100 nm.

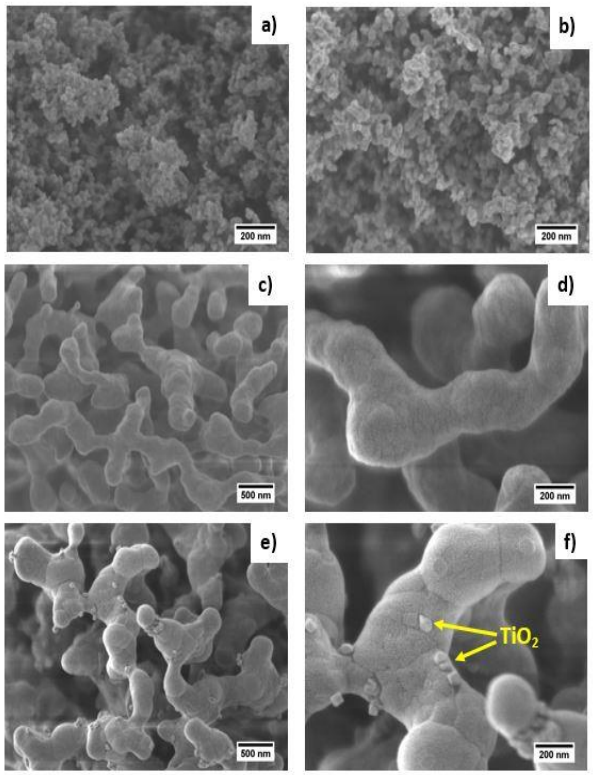

Fig. 6. SEM images of pure SiO_2 support (a), TiO_2/SiO_2 (b), Na_2WO_4/SiO_2 (c, d), and Na_2WO_4-TiO_2/SiO_2 (e, f).

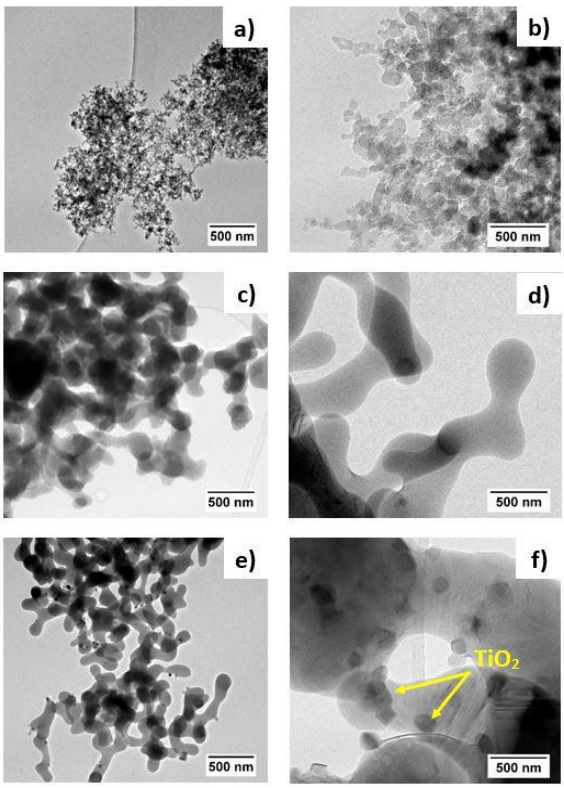

Fig. 7. TEM images of TiO_2/SiO_2 (a, b), Na_2WO_4/SiO_2 (c, d), and Na_2WO_4-TiO_2/SiO_2 (e, f).

The BET surface areas, pore sizes, and pore volumes of the catalysts were measured using an N_2-sorption analyzer. For comparison, the commercial SiO_2 support (surface area of 85–115 m^2/g, amorphous fumed silica, Alfa Aesar) was also dried and calcined using the same method as the catalyst preparation without adding any metal precursors and conducting the BET measurement. As presented in Table 1 and Fig. 8, the isotherm plot of the SiO_2 support was similar to that of the TiO_2/SiO_2 catalyst, in which no hysteretic loop was observed. This indicated that the SiO_2 support and the TiO_2/SiO_2 catalyst are non-porous material, and thus their porous sizes and volumes must have been created from the inter-particles. However, the surface area of the SiO_2 support was lower than that of the TiO_2/SiO_2 catalyst, suggesting that the TiO_2 particles potentially deposited on the surface of SiO_2 and create new surfaces, and thus the surface area of the TiO_2/SiO_2 catalyst increased. The surface areas of the Na_2WO_4/SiO_2 and Na_2WO_4-TiO_2/SiO_2 catalysts were much lower than those of the SiO_2 support and the TiO_2/SiO_2 catalyst. This was consistent with the observations from using the FE-SEM (Fig. 6.) & TEM (Fig. 7.) images, in which the particle sizes of the catalysts containing Na_2WO_4 were larger than those of the TiO_2 catalyst. The hysteretic loops of the Na_2WO_4/SiO_2 and Na_2WO_4-TiO_2/SiO_2 catalysts were similar, in which the pore sizes and the pore volumes generated from the intra-particles and the pore sizes were classified as a meso-porous material. Although the Na_2WO_4-TiO_2/SiO_2 catalyst had a quite small specific surface area, this catalyst had the highest C_{2+} yield, indicating that the synergistic catalyst effect or the selected active components plays a significant role in the catalytic performance.

Table 1. BET surface area (S.A.), pore size, and pore volume of TiO_2/SiO_2, Na_2WO_4/SiO_2, and Na_2WO_4-TiO_2/SiO_2 compared with pure SiO_2 support.

Material	**S.A. (m^2/g)**	**Pore size (nm)**	**Pore volume (cm^3/g)**
SiO_2	86.5	22.2	0.480
Na_2WO_4 / SiO_2	6.5	9.1	0.015
TiO_2 / SiO_2	106.2	17.5	0.460
Na_2WO_4-TiO_2/ SiO_2	5.4	10.0	0.013

The FT-IR patterns of the catalysts are presented in Fig. 9. All three catalysts displayed the Si—O—Si rocking, the Si—O—Si bending, and the Si—O—Si stretching peaks appearing around 490, 800, and 1100 cm^{-1}, respectively. There was one different peak appearing at 621 cm^{-1} for Na_2WO_4-TiO_2/SiO_2 and Na_2WO_4/SiO_2, specifying the existence of α-cristobalite [19] in these two catalysts, in good agreement with the findings in Fig. 5. As can be seen by the catalyst activities presented in Fig. 1, the Na_2WO_4-TiO_2/SiO_2 catalyst had a C_{2+} yield greater than those of the two single catalysts. Thus, one of the important keys that can be considered to improve the C_{2+} yield is to have a catalyst consisting of α-cristobalite interacting with an active crystalline metal oxide.

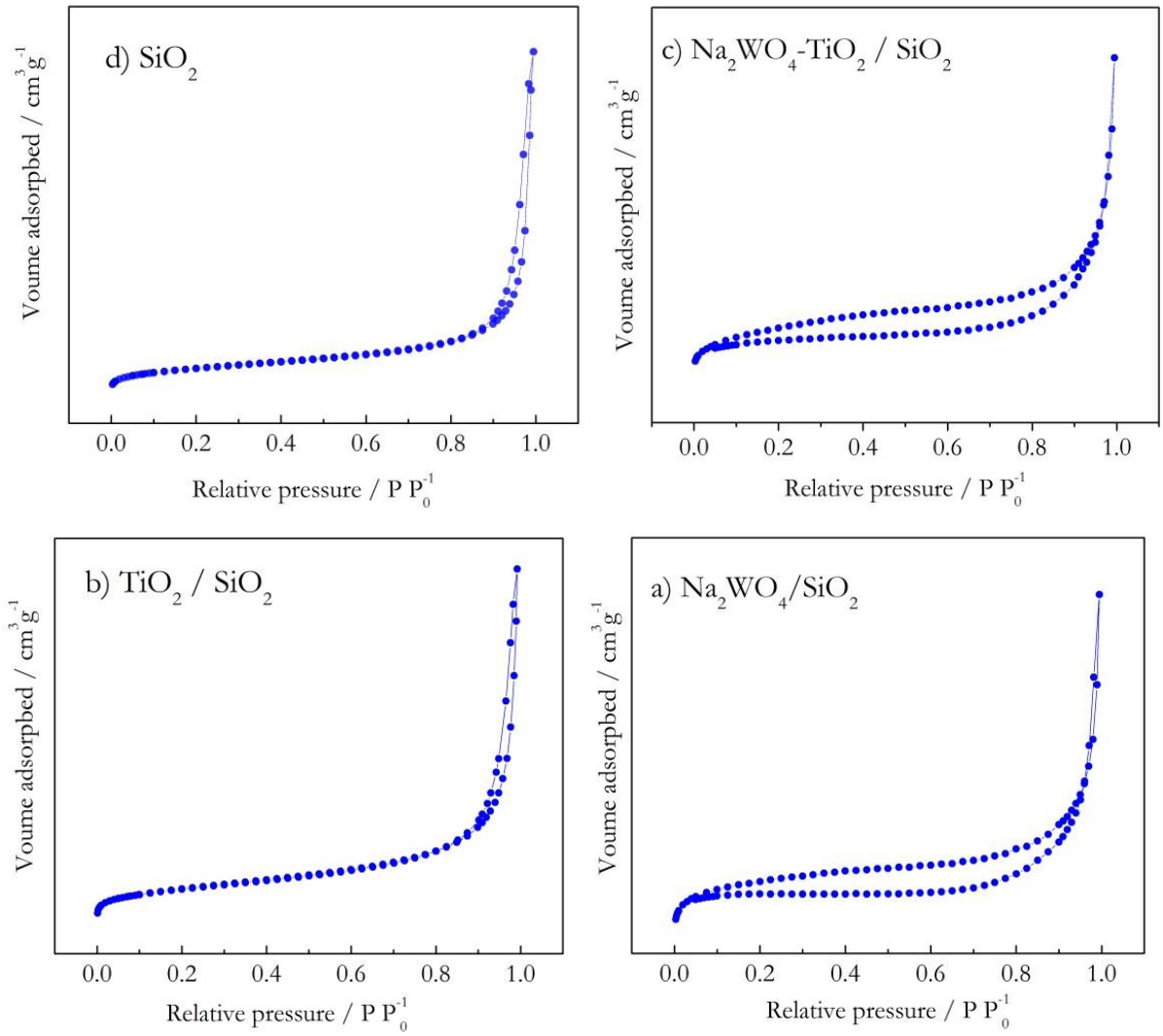

Fig. 8. Isotherm plots of (a) Na_2WO_4/SiO_2 catalyst, (b) TiO_2/SiO_2 catalyst, (c) Na_2WO_4-TiO_2/SiO_2 catalyst, and (d) pure SiO_2 support.

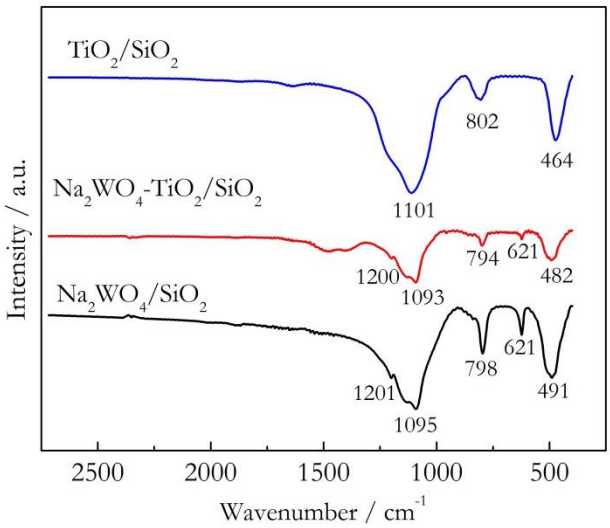

Fig. 9. FT-IR spectra of Na_2WO_4-Ti/SiO_2, Na_2WO_4/SiO_2, and TiO_2/SiO_2 catalysts.

Figure 10 presents the XPS spectra of the catalysts. The XPS scans were carried out in the range of the Na, W, and Ti regions. The observed peaks corresponded to Na_2O (1s = 1071.5 eV) WO_4^{2-}($4f_{5/2}$ = 37.6 eV, $4f_{7/2}$ = 35.3 eV) for Na_2WO_4/SiO_2 and ($4f_{5/2}$ = 37.8 eV, $4f_{7/2}$ = 35.3 eV) for Na_2WO_4-TiO_2/SiO_2, and TiO_2 ($2p_{3/2}$ = 464.2 eV, $2p_{1/2}$ = 459.2 eV) for TiO_2/SiO_2 and ($2p_{3/2}$ = 464.5 eV, $2p_{1/2}$ = 458.8 eV) for Na_2WO_4-TiO_2/SiO_2. Of interest was that the peaks of $WO_4^{2-}$and TiO_2 shifted toward a higher binding energy when Na_2WO_4 and TiO_2 were present in the same catalyst. This was because the Ti or W species are more likely to attach to WO_4^{-2} or O^{2-} bonding with Ti, which is an electron withdrawing group. Thus, the oxidation state of Ti or W has a higher positive charge, and thus shifts in the binding energies can be observed.

Catalyst reducibility and the interaction between the active catalysts and the support were examined using the H_2-TPR technique (see Fig. 11). For the TiO_2/SiO_2 catalyst, no clear H_2 reduction peak could be seen in this temperature range, consistent with previous reports [21, 22]. For Na_2WO_4/SiO_2, a broad reduction peak starting from 450 ºC to above 900 ºC with a maximum H_2 consumption at about 800 ºC was observed, indicating the reduction of W species [22]. The reduction behavior of the Na_2WO_4-TiO_2/SiO_2 catalyst was related to that of the Na_2WO_4/SiO_2 catalyst. However, the starting reduction temperature and the maximum temperature of the Na_2WO_4-TiO_2/SiO_2 catalyst shifted toward a higher temperature (approximately 50 ºC greater than those of the Na_2WO_4/SiO_2 catalyst). This suggested that the redox properties of these metal species substantially change, probably because there is a strong interaction between the WO_4^{2-} component and the TiO_2 crystals [22].

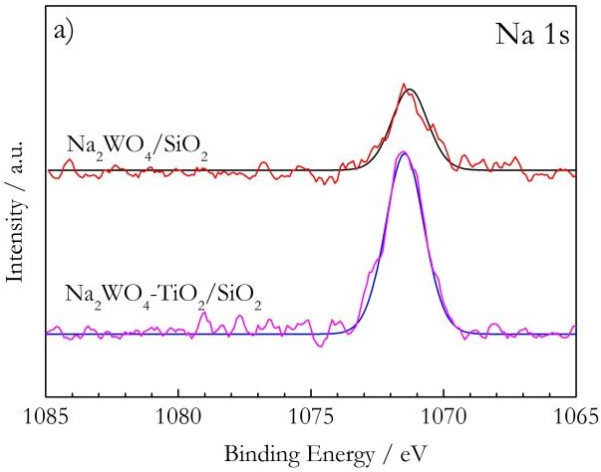

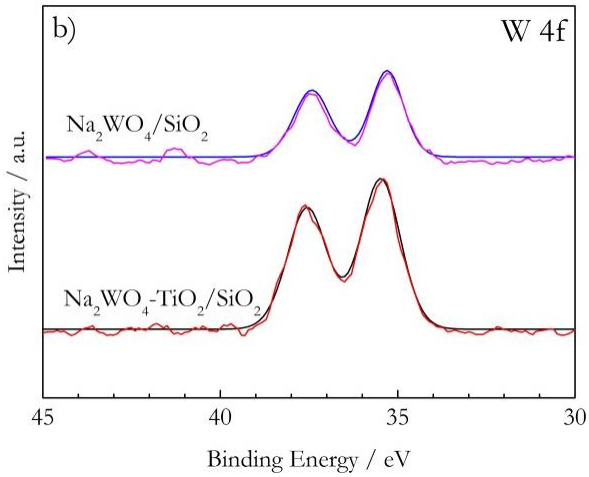

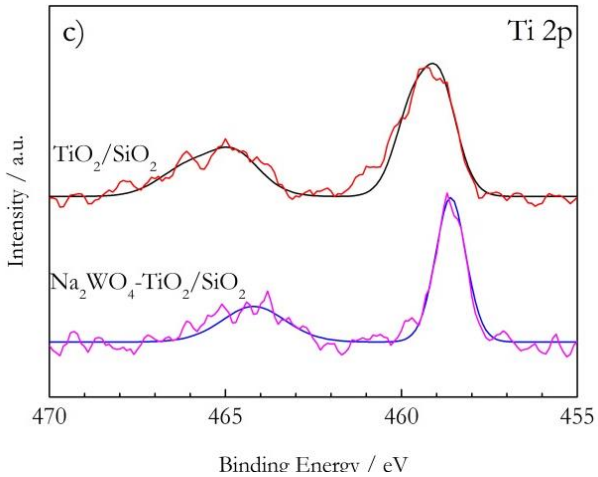

Fig. 10. XPS spectra of Na_2WO_4-Ti/SiO_2, Na_2WO_4/SiO_2, and TiO_2 /SiO_2 showing scanning in the (a) Na, (b) W, and (c) Ti ranges.

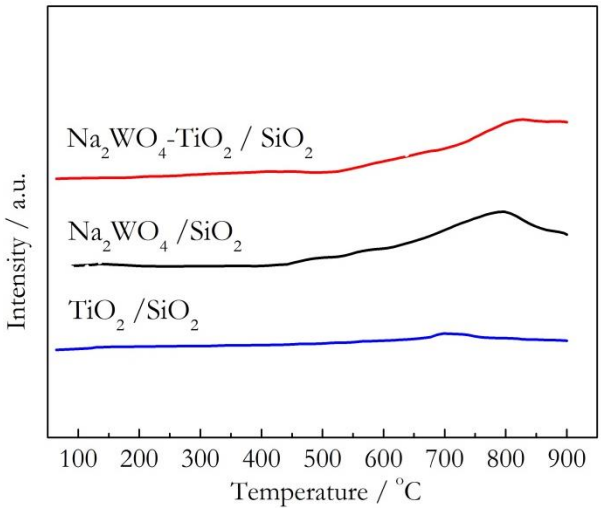

Fig. 11. H_2-TPR patterns of Na_2WO_4-TiO_2/SiO_2, Na_2WO_4/ SiO_2, and TiO_2/SiO_2.

In previous reports on the activity of catalysts containing Na_2WO_4 and SiO_2 for OCM reaction, there have been some suggestions about the enhancement of those catalysts as follows. Ji, et al. stated that the existence of the α-cristobalite phase was a critical necessity for the C_{2+} formation of catalysts containing Na_2WO_4 and SiO_2 for OCM reaction [9]. Elkins, et al. claimed that the interaction between the α-cristobalite structure and the WO_4^{2-} tetrahedron structure was crucial in the generation of C_{2+} and the inter-phase between these two components was the active surface species. Moreover, the WO_4^{2-} tetrahedron could stabilize the Mn_2O_3 and Na_2WO_4 phases, so that the catalysts could maintain their high activity during the reaction [23]. Furthermore, Palermo, et al. suggested that Na played dual roles in promoting the activity of MnO_x-Na_2WO_4/SiO_2 catalysts by acting as both a chemical and a structural promoter [24, 25]. From these reports, it can be certainly claimed that the presence of the α-cristobalite structure, the crystalline Na_2WO_4, and the anatase-TiO_2 crystals in the Na_2WO_4-TiO_2/SiO_2 catalyst strongly enhances the activity of the catalyst and is crucial for the formation of C_{2+} in the reaction.

4. Conclusions

The combination of 5wt% TiO_2 and 5wt% Na_2WO_4 on SiO_2 support (i.e. Na_2WO_4-TiO_2), prepared using the co-impregnation method, was superior to the single catalysts of its component (i.e. Na_2WO_4/SiO_2, TiO_2/SiO_2). In studying the operating conditions by co-feeding N_2 gas as a diluent gas into the reactant

gases at different volume ratios and different temperatures, the maximum C_{2+} yield was found at an $N_2/(4CH_4:1O_2)$ feeding gas ratio 1:1 by volume and at 700 ºC. The Na_2WO_4-TiO_2 catalyst produced the highest C_{2+} yield at 4.9% with 71.7% C_{2+} selectivity and 6.8% CH_4 conversion under these optimal operating conditions. Furthermore, the activity of the catalyst had good stability over 24 h of testing. Characterization of the Na_2WO_4-TiO_2 catalyst using XRD and FT-IR showed that α-cristobalite and crystalline anatase-TiO_2 were present. These two crystal components played a significant role in the formation of C_{2+} for the OCM reaction. The FE-SEM, TEM, and BET results were in good agreement with the findings of the XRD and FT-IR analyses. Of great interest for future study is the analysis of the kinetic mechanism of the catalyst for OCM reaction or improvement of the catalyst activity by adding promoters.

Acknowledgements

We would like to thanks the Thailand Research Fund and the Commission on Higher Education (grant numbers IRG5980004 & MRG6180232); the National Nanotechnology Center (NANOTEC), NSTDA, Ministry of Science and Technology, Thailand, through its program of Research Network NANOTEC (RNN); the Center of Excellence on Petrochemical and Materials Technology; the Kasetsart University Research and Development Institute (KURDI); and the Department of Chemical Engineering and the Faculty of Engineering at Kasetsart University for financial supports. P. Kidamorn received funding through a scholarship from the Faculty of Engineering at Kasetsart University.

References

[1] G. J. Hutchings, M. S. Scurrell, and J. R. Woodhouse, "Oxidative coupling of methane using oxide catalyst," *Chem. Soc. Rev.*, vol. 18, pp. 251-283, 1989.

[2] M. Y. Sinev, Z. T. Fattakhova, V. I. Lomonosov, and Y. A. Fordienko, "Kinetics of oxidative coupling of methane: bridging the gap between comprehension and description," *J. Nat. Gas Chem.*, vol. 18, pp. 273-287, 2009.

[3] K. Khammona, S. Assabumrungrat, and W. Wiyarath, "Reviews on coupling of methane over catalysts for application in C_2 hydrocarbon production," *J. Eng. Appl. Sci.*, vol. 7, pp. 447-455, 2012.

[4] S. M. K. Shahri and A. N. Pour, "Ce-promoted Mn/Na_2WO_4/SiO_2 catalyst for oxidative coupling of methane at atmospheric pressure," *J. Nat. Gas Chem*, vol. 19, pp. 47-53, 2010.

[5] R. Mariscal, M. A. Pena, and J. L. G. Fierro, "Promoter effects of dichloromethane on the oxidative coupling of methane over MnMgO catalysts," *Appl. Catal., A*, vol. 131, pp. 243-261, 1995.

[6] V. R. Choudhary, V. H. Rane, and S. T. Chaudhari, "Factors influencing activity/selectivity of La-promoted MgO catalyst prepared from La- and Mg- acetates for oxidative coupling of methane," *Fuel*, vol. 79, pp. 1487-1491, 2000.

[7] Z. Gholipour, A. Malekzadeh, R. Hatami, Y. Mortazavi, and A. Khodadadi,"Oxidative coupling of methane over (Na_2WO_4+Mn or Ce)/SiO_2 catalysts: In situ measurement of electrical conductivity," *J. Nat. Gas Chem*, vol. 19, pp. 35-42, 2010.

[8] R. T. Yunarti, M. Lee, Y. J. Hwang, D. J. Suh, J. Lee, I. W. Kim, and J. M. Ha, "Transition metal-doped TiO_2 nanowire catalysts for the oxidative coupling of methane," *Catal. Commun*, vol. 50, pp. 54-58, 2014.

[9] S. Ji, T. Xiao, S. Li, L. Chou, B. Zhang, C. Xu, R. Hou, A. P. E. York, and M. L. H Green, "Surface WO_4 tetrahedron: The essence of the oxidative coupling of methane over M-W-Mn/SiO_2 catalysts," *J. Catal.*, vol. 220, pp. 47-56, 2003.

[10] J. Y. Lee, W. Jeon, J. W. Choi, Y. W. Suh, J. M. Ha, D. J. Suh, and Y. K. Park, "Scaled-up production of C_2 hydrocarbons by the oxidative coupling of methane over pelletized Na_2WO_4/Mn/SiO_2 catalysts: Observing hot spots for the selective process," *Fuel.*, vol. 106, pp. 851-857, 2013.

[11] A. Malekzadeh, A. Khodadadi, A. K. Dalai, and M. Abedini, "Oxidative coupling of methane over Lithium doped (Mn+W)/SiO_2 catalysts," *J. Nat. Gas Chem*, vol. 16, pp. 121-129, 2007.

[12] J. Wang, L. Chou, B. Zhang, H. Song, J. Zhao, J. Yang, and S. Li, "Comparative study on oxidation of methane to ethane and ethylene over Na_2WO_4-Mn/SiO_2 catalysts prepared by different methods," *J. Mol. Catal. Chem.*, vol. 245, pp. 272-277, 2006.

[13] N. Hiyoshi and T. Ikeda, "Oxidative coupling of methane over alkali chloride-Mn-Na_2WO_4/SiO_2 catalysts: Promoting effect of molten alkali chloride," *Fuel Process. Technol.,* vol. 133, pp. 29-34, 2015.
[14] T. W. Elkins and H. E. Hagelin-Weaver, "Characterization of Mn-Na_2WO_4/SiO_2 and Mn-Na_2WO_4/MgO catalysts for the oxidative coupling of methane," *Appl. Catal., A*, vol. 497, pp. 96-106, 2015.
[15] F. Papa, D. Gingasu, L. Patron, A. Miyazaki, and I. Balint, "On the nature of active sites and catalytic activity for OCM reaction of alkaline-earth oxides-neodymia catalytic systems," *Appl. Catal., A,* vol. 375, pp. 172-178, 2010.
[16] V. H. Rane, S. T. Chaudhari, and V. R. Choudhary, "Oxidative coupling of methane over La-promoted CaO catalysts: Influence of precursors and catalyst preparation method," *J. Nat. Gas Chem.*, vol. 19, pp. 25-30, 2010.
[17] D. J. Wang, M. P. Rosynek, and J. H. Lunsford, "Oxidative coupling of methane over oxide-supported sodium-manganese catalysts," *J. Catal.*, vol. 155, pp. 390-402, 1995.
[18] F. Basile, G. Fornasari, F. Trifiro, and A. Vaccari, "Partial oxidation of methane: Effect of reaction parameters and catalyst composition on the thermal profile and heat distribution," *Catal. Today*, vol. 64, pp. 21-30, 2001.
[19] S. Ji, T. Xiao, S. Li, L. Chou, B. Zhang, C. Xu, R. Hou, A. P. E York, and M. L. H Green, "Surface WO_4 tetrahedron: the essence of the oxidative coupling of methane over M·W·Mn/SiO_2 catalysts," *J. Catal.*, vol. 220, pp. 47-56, 2003.
[20] A. M. Venezia, F. Raimondi, V. La Parola, and G. Deganello, "Influence of sodium on the structure and HDS activity of Co-Mo catalysts supported on silica and aluminosilicate," *J. Catal.*, vol. 194, pp. 393-400, 2000.
[21] T. Chukeaw, A. Seubsai, P. Phon-in, K. Charoen, T. Witoon, W. Donphai, P. Parpainainar, M. Chareonpanich, D. Noon, B. Zohour, and S. Senkan, "Multimetallic catalysts of RuO_2–CuO–Cs_2O–TiO_2/SiO_2 for direct gas-phase epoxidation of propylene to propylene oxide," *RSC Adv.*, vol. 6, pp. 56116-56126, 2016.
[22] J. Li, G. Lu, G. Wu, D. Mao, Y. Guo, Y. Wang, and Y.Guo, "Effect of TiO_2 crystal structure on the catalytic performance of Co_3O_4/TiO_2 catalyst for low-temperature CO oxidation," *Catal. Sci. Technol.*, vol. 4, pp. 1268-1275, 2014.
[23] T. W. Elkins, and H. E. Hagelin-Weaver, "Characterization of Mn-Na_2WO_4/SiO_2 and Mn-Na_2WO_4/MgO catalysts for the oxidative coupling of methane," *Appl. Catal., A*, vol. 497, pp. 96-106, 2015.
[24] A. Palermo, J. P. H Vazquez, A. F. Lee, M. S. Tikhov, and R. M. Lambert, "Critical influence of the amorphous silica-to-cristobalite phase transition on the performance of Mn/Na_2WO_4/SiO_2 catalysts for the oxidative coupling of methane," *J. Catal.*, vol. 177, pp. 259-266, 1998.
[25] Y. T. Chua, A. R. Mohamed, and S. Bhatia, "Oxidative coupling of methane for the production of ethylene over sodium-tungsten-manganese-supported-silica catalyst (Na-W-Mn/SiO_2)," *Appl. Catal., A*, vol. 343, pp. 142-148, 2008.